Influence of order–disorder parameters on the reducibility of Ni- and Cu-containing silicates: application to talc and chrysocolla

J.Y. Carriat, M. Che, M. Kermarec[1]

Laboratoire de Réactivité de Surface et Structure, URA 1106 CNRS,
4 place Jussieu, 75252 Paris Cedex 05, France

and

A. Decarreau

Laboratoire de Pétrologie de la Surface, Université de Poitiers,
avenue du Recteur Pineau, 86022 Poitiers Cedex, France

Received 10 May 1993; accepted 23 November 1993

Reference phyllosilicates (Ni-talcs and chrysocolla) have been synthesized with the aim of identifying supported layered silicates in the preparation of Ni/SiO_2 and Cu/SiO_2 materials. The analysis of temperature programmed reduction (TPR) profiles and X-ray diffraction (XRD) patterns of talc synthesized at different temperatures shows a strong influence of the crystallinity of the Ni silicate on its reducibility. Chrysocolla remains ill-crystallized whatever the temperature of synthesis. The reducibility of the two silicates is discussed in terms of the structure of the silicate and the reducibility of the transition metal-ion. The asymmetric shape of the TPR curves of Ni-talcs is interpreted on the basis of the phase-boundary controlled model and the presence of a heterogeneous particle size distribution. The results emphasize the role of the crystallinity and show that the identification of supported silicate phases from TPR only may not be reliable.

Keywords: TPR; crystallinity; Ni-talc; chrysocolla

1. Introduction

Supported transition metal ion catalysts constitute an important class of catalysts. It is now well known that the preparation method induces various roles for the support leading to different ion–support interactions [1]. Earlier work on the characterization of silica-supported Ni catalysts prepared by precipitation meth-

---

[1] To whom correspondence should be addressed.

ods [2–5] and by ion exchanges [6,7] showed a strong interaction between silica and Ni^{2+} ions, suggesting the formation of Ni silicate layers on silica. Recently, EXAFS spectroscopy was shown to be a powerful tool to identify a Ni layer silicate in these catalysts prepared by ion exchange, impregnation or deposition–precipitation [8,9]. The nature and the organization of the supported phase influence the behaviour of the precursor during calcination and reduction pretreatments and contribute to determine the size and dispersion of the metallic particles, which strongly affect the catalytic properties. Recently, the ability to prepare Ni species with controlled interactions with silica was used to produce, in a two-step procedure, supported metallic Ni particles of a given size [10].

Temperature programmed reduction (TPR) profiles have recently been used as fingerprints of the interaction of the metal ion with the support [11]: the stronger the interaction, the higher the temperature of the TPR peak. In the case of silica-supported copper catalysts, TPR was used to identify a silicate phase by comparison with mineral copper silicates of known structure [12]. In that work, supported copper silicates were identified as chrysocolla-like phases, for catalysts prepared by ion exchange and deposition–precipitation. In a subsequent paper, the identification of the supported silicate as chrysocolla (Cu-containing silicate) was confirmed by diffuse reflectance infrared Fourier-transform (DRIFT) spectroscopy [13].

Synthetic Ni-talc and antigorite [14] (2 : 1 and 1 : 1 phyllosilicates respectively, see description in section 3) were used as references for the identification of different phases in natural hydrous Ni-containing silicates, studied by XRD and TPR [15]. The thermal stability of those synthetic materials has been related to their crystallinity. However, this parameter has never been taken into account in the characterization of supported silicates.

Because mineral compounds often contain impurities, their use as reference compounds may appear questionable. This is the reason why we have synthesized pure Ni 2 : 1 and 1 : 1 phyllosilicates (referred to as Ni-talcs and nepouites) with various degrees of crystallinity, in order to identify the silicates produced in the preparation of silica-supported Ni catalysts. A Cu-containing silicate of another structure (chrysocolla) was also synthesized with the same objective and compared to the natural mineral.

The crystallinity of Ni-talc and chrysocolla was controlled by XRD while their reducibility was investigated using the TPR technique. This paper reports on the dependence of the reducibility of those synthetic materials on their crystallinity and points out the ambiguity of identifying silica supported silicates on the basis of TPR only.

2. Structure of the phyllosilicates

The structure of 2 : 1 (TOT) and 1 : 1 (TO) phyllosilicates which are layered silicates, is well known and was extensively described by Brindley and Brown [16a].

The layer of Ni-talc corresponding to the formula $Si_4Ni_3O_{10}(OH)_2$, is composed of an octahedral (O) sheet linked to two tetrahedral (T) sheets while the layer of nepouite (serpentine-like mineral of TO structure) is composed of an octahedral sheet linked to an adjacent tetrahedral sheet (figs. 1a and 1b respectively). The tetrahedra are occupied by Si atoms and the octahedra by Ni atoms.

Natural samples of chrysocolla are poorly ordered 1 : 1 or TO layered silicates containing Cu and Al ions [16b]. The precise crystal structure is not well established [17,18]. The structure described by Van Oosterwyck-Gastuche [18] shows alternate corrugated sheets of SiO_4 tetrahedra and discontinuous sheets of Cu octahedra (fig. 1c).

3. Experimental

Synthetic clays were obtained following a process described in detail elsewhere [19,20]. The initial step of the synthesis consists in a coprecipitation of a silicometallic gel according to the reactions:

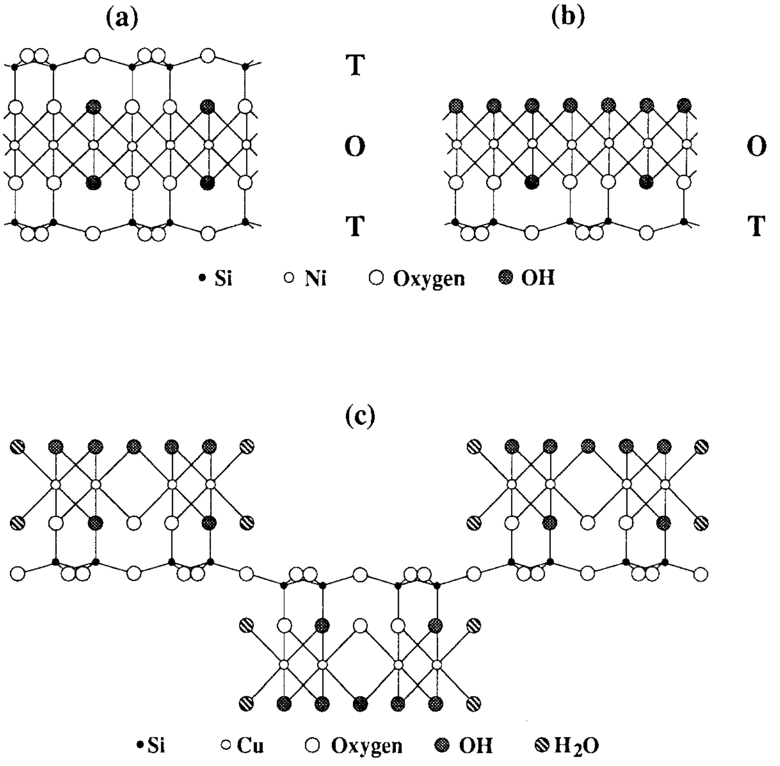

Fig. 1. Projection onto the *bc* plane of a TOT layer of Ni-talc (a), a TO layer of nepouite (b), a TO layer in the proposed structure for chrysocolla [18] (c).

for Ni-talcs:

$$4SiO_2Na_2O + 3NiCl_2 + 2HCl \rightarrow Si_4Ni_3O_{10}(OH)_2 + 8NaCl\,,$$

for nepouite:

$$2SiO_2Na_2O + 3NiCl_2 + 2NaOH \rightarrow Si_2Ni_3O_5(OH)_4 + 6NaCl\,,$$

for chrysocolla:

$$2SiO_2Na_2O + 2CuCl_2 + H_2O \rightarrow Cu_2Si_2O_5(OH)_2 + 4NaCl\,.$$

Gels were then hydrothermally treated for two weeks at temperatures ranging from 25 to 500°C for Ni-talcs and Ni-serpentines, and at 25 and 80°C for chrysocolla. Ni-talcs synthesized at 25, 150, 250 and 500°C are referred to as Ta_{25}, Ta_{150}, Ta_{250} and Ta_{500} respectively. This synthesis procedure was shown to produce one phase, i.e., the given clay mineral. Thus samples quenched at the earlier stage of the coprecipitation were constituted of germs of the clay mineral only (the average crystallite size growing with time of synthesis) [19,20].

X-ray diffraction (XRD) patterns were recorded with a Phillips diffractometer using a Ni filtered Co $K\alpha_1$ radiation selected by a quartz monochromator. The rate of recording was 1° $2\theta\,\mathrm{min}^{-1}$.

The reducibility of the synthesized materials was investigated using the temperature programmed reduction technique (TPR). The samples (about 10 mg in weight) were placed in a thin bed in a microreactor and reduced up to 900°C under a 5% H_2/Ar mixture at a 25 ml min^{-1} (23.1 ml min^{-1} NTP) flow rate and a heating ramp of 7.5°C min^{-1}. The TPR microreactor was computer interfaced in our laboratory. The hydrogen consumption, based on area under the TPR curve, was detected by the thermal conductivity cell of a catharometer. Separate lines of a 5% H_2/Ar mixture at the same controlled flow rate (25 ml min^{-1}) were used for each compartment (reference and measurement) of the catharometer. The calibration was done with Ar, by switching, at the end of the TPR experiment, the 5% H_2/Ar mixture in the measurement line to pure Ar (the surface of the resulting square peak recorded for a given time corresponding to the concentration of the 5% H_2/Ar mixture during this time). The error on H_2 consumption was estimated to be about 10%. The TPR profiles have been normalized to the Ni weight. The reduction degree α was estimated from the ratio of the hydrogen consumption to the amount of Ni present in the sample (taking into account the total amount of water). This estimation was cross-checked with CuO.

4. Results and discussion

4.1. Ni-TALCS

The XRD patterns show that the crystallinity of the clay mineral increases with the temperature of synthesis (figs. 2a–2d). Ni-clays synthesized at 25°C consist of

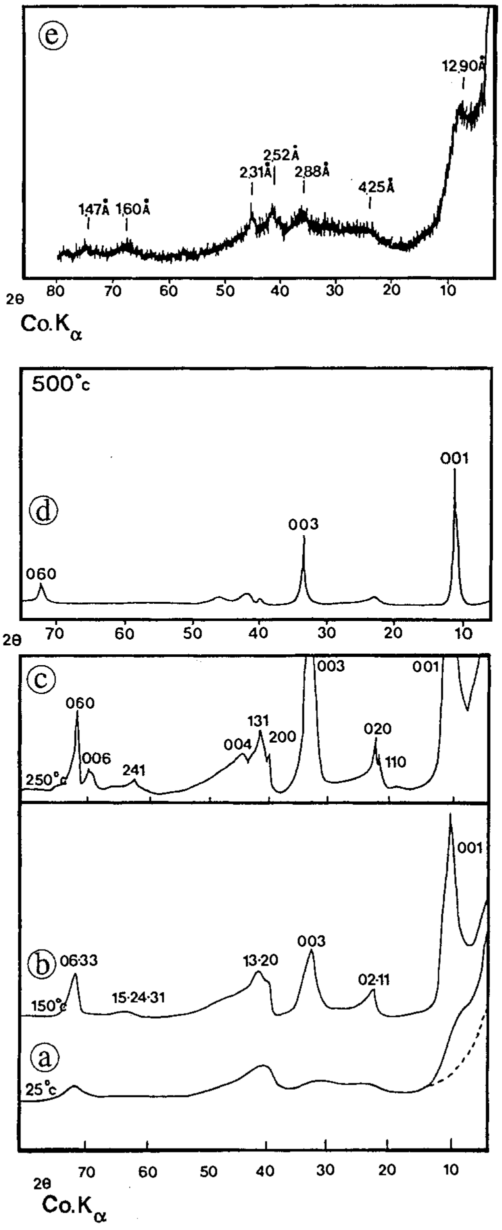

Fig. 2. X-ray powder diffraction patterns of talcs synthesized at (a) 25°C, (b) 150°C, (c) 250°C, (d) 500°C and chrysocolla synthesized at (e) 80°C. (For talcs, the magnification of the intensity scale is proportional to: 1 (500°C) and 6 (25, 150 and 250°C).

Ni-talc layers regularly intercalated with water molecules (H_2O : Si ratio = 2 : 4). The structure is turbostratic, i.e., talc layers are stacked with random rotation and/or displacement stacking faults. Therefore XRD patterns exhibit only a (001) basal reflection and (*hk*0) reflections (biperiodic structure) for samples synthesized in the 25–100°C temperature range. Thus, the (001) reflection appears as a broad shoulder for samples synthesized at 25°C (fig. 2a). When the temperature of synthesis increases, stacking faults are less numerous and the water content decreases. For clays synthesized at 150°C ($H_2O : Si = 0.5 : 4$), a few *hkl* reflections are observed. The 001 and 003 lines sharpen while asymmetric lines are still observed for (*hk*0) reflections (fig. 2b). For samples synthesized in the 170–250°C range, XRD patterns show *hkl* reflections indicating thus a triperiodic structure (fig. 2c). These materials are almost completely dehydrated. Talc synthesized at 500°C is perfectly crystallized as shown by intense symmetric lines (fig. 2d) (the magnification scale chosen allows the observation of (001) and (*hk*0) reflections only).

The crystal size (crystal size coherency) in a direction parallel to the (001) layer plane, was estimated from the Scherrer formula: $L = K\lambda/B \cos\theta$, applied to the (060) and (330) reflections for samples synthesized in the 25–500°C range. The K value was fixed to 0.9 as usual in clay studies [16c]. The number of stacked layers was estimated from the peak broadening of the (001) reflections, assuming the absence of interstratification faults (table 1). This hypothesis seems reliable since similar values for the number of stacked layers were found from TEM measurements on ultra thin cuts. The number of stacked layers associated within one clay particle is shown to increase with the temperature of synthesis (table 1). The average particle size measured by TEM is greater than the corresponding crystal size coherency and grows with improved crystallinity.

Fig. 3 exhibits the TPR profiles of Ni-talc synthesized at 25, 150, 250 and 500°C. The corresponding maxima of the TPR peaks are observed at 470, 668, 745 and 846°C respectively. The better the crystallinity, the higher the TPR peak. For the lowest temperature of synthesis (25°C), the low crystallinity in the (a, b) plane may indicate that the silica tetrahedra do not form extended sheets and therefore incompletely shield the Ni octahedral sheet, leading thus to an easier reducibility of Ni as shown by the TPR maximum at 470°C. However, it can be noticed that the existence of local silicate structure even ill-organized, keeps this TPR maximum (470°C) far above that of $Ni(OH)_2$ which is observed at about 300°C [8,15].

Asymmetric profiles are registered for all silicates which present a tail towards

Table 1
X-ray data for synthesized Ni-talcs

Synthesis temperature (°C)	Crystal size[a] (Å±5%)	Average number of stacked layers[b] (±1)
25	25	2
80	50	4
150	85	7
250	310	11
500	580	33

[a] The crystal size was estimated from the (060) and the (330) reflections, which corresponds to a crystalline coherency range in a direction parallel to the layer planes.

[b] Estimated from the (001) reflection.

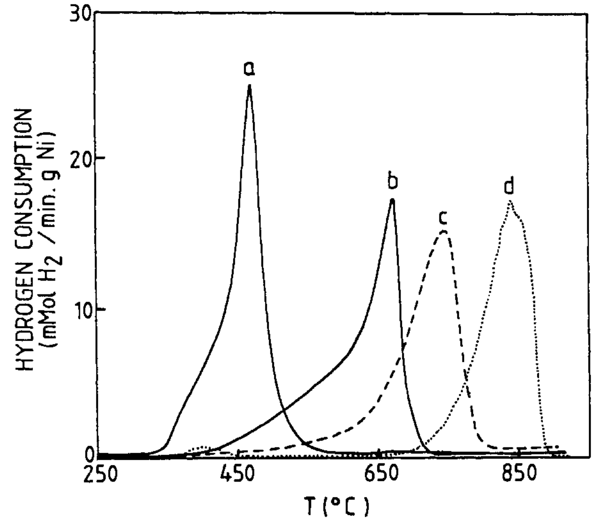

Fig. 3. TPR profiles of Ni-talc synthesized at (a) 25°C, (b) 150°C, (c) 250°C, (d) 500°C.

lower temperatures (fig. 3). The TPR curve of Ta_{500} is composed of a very weak peak around 400°C (the origin of which is not clear) and a sharp peak at 846°C. Its profile is more symmetric and presents a shoulder towards higher temperatures (fig. 3d). The full width at half maximum increases with the temperature of synthesis up to 250°C then remains constant up to 500°C. Table 2 displays the data concerning these profiles.

For interfacial processes, Lemaitre [21], in agreement with earlier work [22,23], proposed two main reaction models: the phase boundary-controlled reaction model and the nucleation-controlled reaction model. Theoretical TPR curves have been calculated for both models and for the latter one, quite symmetric peaks shifted towards lower temperatures with increasing particle size are observed.

Table 2
TPR data for synthesized Ni-talcs [a,b] and natural Ni-kerolite [b]

Material	Weight (mg)	Full width at half height (°C)	Maxima of TPR peaks (°C)	Onset of reduction (°C)	Δ^{d} (°C)
Ta_{25} [a]	9.5	44	470	325	145
Ta_{150} [a]	10.6	62	668	380	288
Ta_{250} [a]	10.1	78	745	420	325
Ta_{500} [a]	11.2	78	846, sh 851	625	216
Ta_{350} [b]	10.8	170	780, 830	475	
Ni-kerolite [c]	23	170	730, 800		

[a] This work.

[b] Ni-talc synthesized by Martin et al. [14] and studied by Lemaitre and Gérard [15].

[c] Natural mineral studied by Lemaitre and Gérard [15].

[d] Temperature shift between the maximum of the TPR peak and the onset of the reduction.

Thus, this model is not consistent with our results (peaks shifted towards higher temperatures with increasing particle size) since improving the crystallinity increases the crystal size coherency and therefore the average particle size (table 2).

In the phase boundary-controlled reaction model, the interfacial reaction moves towards the bulk of the solid along one, two or three directions and the reaction rate is assumed to be proportional to the surface area of the unreacted particle. This model, applied to a single particle size, gives TPR shapes with tailing towards lower temperatures. It was shown that increasing the particle size led to broader peaks shifted towards higher temperatures with decreased intensities. These trends could be consistent with the profiles observed for the first three talcs of the series (figs. 3a–3c).

The experimental profiles could fit an interfacial front of reaction moving along two or three directions [21]. The question which now arises is whether the crystallinity influences the preferential routes for hydrogen. For layered structures, the obvious routes for hydrogen correspond to the layer planes and/or the *c* axis. The accessibility of octahedral Ni^{2+} ions to hydrogen proceeds from the destruction of OH groups (constitutional OH groups which are perpendicular to the layer plane and edge OH groups at the boundaries of the particle). Although the contribution of these two populations is strongly dependent on the crystallinity (poorly crystallized particles exhibit a larger fraction of edge OH groups than well crystallized particles), the transport of hydrogen along the *c* axis, after destruction of the constitutional OH groups, seems improbable since, once constitutional OH groups are attacked, hydrogen must pass through the barrier of SiO_4 tetrahedra before reaching the next octahedral layer. Whatever the crystallinity degree, edge OH groups are immediately accessible and more reactive than constitutional OH groups. After the destruction of edge OH groups localized at the external octahedra, it is possible to speculate that the front of the reduction moves towards the core of the particle within the octahedral layer planes through the attack of lattice oxygen atoms. Therefore, the reduction of Ni^{2+} ions requires the collapse of the silicate structure which depends on the degree of crystallinity. Infrared results show that calcination of the phyllosilicate at increasing temperatures leads to progressive dehydroxylation of constitutional OH groups and therefore to the structure breakdown into amorphous silica and NiO [24]. This is shown by the concomitant decrease of ν and δ OH bands of structural OH groups and the appearance of silica SiO bands around 1105 and 800 cm^{-1}. This dehydroxylation process is all the more favoured as the synthesis is performed at lower temperatures. This fact is consistent with the easier reducibility of poorly crystalline talcs corresponding to smaller particle sizes. However, in this case (synthesis at 25°C) the presence of faults facilitates also the passage of hydrogen through the crystal.

From a general point of view, the experimental profiles are more complex than those expected from the boundary-controlled reaction model: thus, slight inflexions are observed on the low temperature side of the TPR curves for Ta_{25} and Ta_{150}.

On the other hand, the existence of a single particle size is unlikely and it may be assumed that there is a particle size distribution. Unfortunately, the particle size distribution function, which may strongly affect the TPR curve is not available from TEM studies since the particles are often associated. Thus, a multimodal size distribution could lead to multiple TPR peaks.

The existence of a continuous distribution of the particle sizes produced during the synthesis may also explain the asymmetric shape of the TPR peak, the asymmetric tail towards lower temperatures corresponding to particles of smaller sizes. The close values observed for the onset of the reduction of the first three talcs of the series (325–420°C) as compared to the shift with the values of the corresponding TPR maxima (Δ values) are consistent with the presence of particles of smaller and comparable sizes which remain even after synthesis at 250°C (table 2). A distribution with a slightly larger fraction of particles of smaller sizes could account for the inflexions found for the TPR profiles of Ta_{25} and Ta_{150}. By contrast, when the synthesis is performed at 500°C, the crystal size coherency increases to the detriment of the particles of smaller size which are no longer observed as shown by the higher value of the onset of the reduction which occurs near 630°C.

One may notice that the method of preparation has a strong influence on the shape of the TPR curve. Thus, Ni-talc and Ni-antigorite (serpentine-like structure), prepared from hydrothermal treatment at 350°C of stoichiometric mechanical mixtures of pure and high surface area $Ni(OH)_2$ and SiO_2 [14], gave rise to a double reduction peak [15]. The maxima for the Ni-talc are observed at 780 and 830°C. A broad peak was registered for Ni-kerolite (talc-like structure) which exhibited a maximum at 730°C and a shoulder around 800°C. Table 2 indicates a full width value at half height of about 170°C for these samples whereas a maximum value of 84°C is found for Ta_{250}. In order to be reliable, this comparison requires that the experiments be carried out under the same conditions. Although the same 5% H_2/Ar mixture and similar sample weights were used, the flow rate and the heating rate were slightly different. We have checked that a weak variation of these parameters does not significantly influence the TPR width, by using the same conditions as those of Lemaitre and Gerard [15] (fig. 4). Therefore, the presence of two maxima for the Ni-talc synthesized by Martin et al. [14] could suggest the existence of a bimodal population of particle sizes of nearly equal number. Our method of synthesis gives rise to a continuous distribution of particle sizes for synthesis performed at temperatures lower than 250°C. At 500°C, a narrower distribution of particle sizes is produced.

Table 3 exhibits the values for the reduction degree (α) of the Ni silicates synthesized at 25, 150, 250 and 500°C respectively. The average value appears close to 75%. In past years, Wendt [25] found a reduction degree of 80% for a Ni-talc prepared by hydrothermal synthesis at 400°C of $Ni(OH)_2$ and SiO_2. One may wonder why these talcs are not completely reduced. Since our equipment did not allow heating beyond 900°C, one may think that the ultimate reduction of the phyllosilicate occurs at temperatures higher than 900°C. Nevertheless, the dependence of the

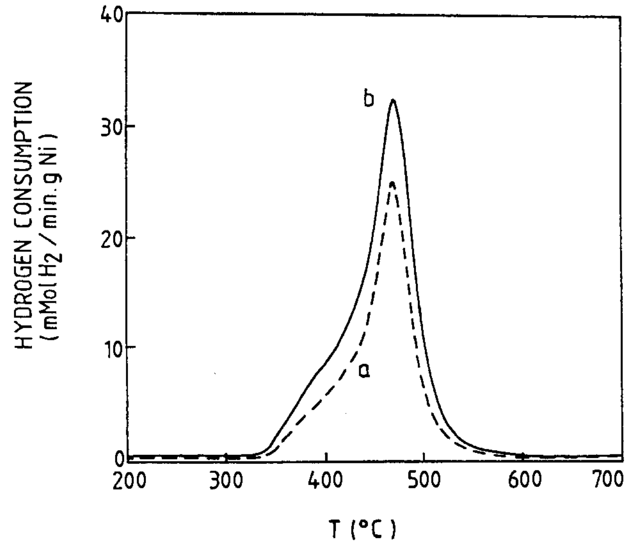

Fig. 4. Influence of the flow-rate f and the heating rate h on the TPR profile of Ta_{25}. (a) $f = 23.1$ ml min^{-1} (NTP), $h = 7.5°C\,min^{-1}$. (b) $f = 35\,ml\,min^{-1}$ (NTP), $h = 10°C\,min^{-1}$.

reducibility of the synthesized materials with the degree of crystallinity is not well accounted for by the single average value found for α (75%), all the more as the reduction of talc synthesized at 25°C (fig. 3a) is achieved at 575°C. One should rather expect decreasing α values with increasing crystallinity. This result prompted us to measure the reduction degree by another method.

After TPR up to 900°C, the sample was purged under flowing Ar and the temperature lowered to 500°C and maintained for 1 h, to eliminate hydrogen chemisorption. The Ni particles were then dissolved and reoxidized by 9 N H_2SO_4 according to the procedure described by Coenen [26], and the hydrogen released

Table 3
Reduction degree (α) estimated from TPR [a]

Sample	Weight (mg)	H_2O	Ni (wt%)	α
Ta_{25}	9.5 41 149	26.1	28	0.77 0.80 0.85
Ta_{150}	10.6 10.8	17.8	31.1	0.66 0.76
Ta_{250}	8.8 10.1	12	33.1	0.73 0.76
Ta_{500}	11.2	7	35.2	0.74

[a] Performed up to 900°C.

measured by volumetry. Unfortunately the sample remained black indicating that the metallic particles were not fully reoxidized, and a value of 50% was found for the reduction degree. The failure of the reoxidation method applied to bulk phyllosilicates arises from the presence after TPR up to 900°C of metallic particles of probably large size, a fraction of which were encapsulated in silica.

4.2. CHRYSOCOLLA

Pure chrysocolla containing only copper was synthesized in the 25–80°C temperature range. Although the degree of crystallinity of the synthetic samples appears to be more important than that of the natural mineral, it still remains low. In contrast to Ni silicates, the XRD patterns showed that the crystallinity was not improved by syntheses performed above 80°C. Fig. 2e shows the XRD diffractogram of chrysocolla synthesized at 80°C.

Fig. 5 exhibits the TPR curves of samples of chrysocolla synthesized at 25 and 80°C. The corresponding maxima are observed at 230 and 276°C respectively. The natural chrysocolla investigated by Van der Grift et al. [12] showed a sharp maximum at 217°C and a broad one at 277°C whereas the synthesized materials exhibited a unique sharp maximum. The existence of two maxima in natural chrysocolla may be due to the heterogeneity of the material, the broad maximum corresponding to a better organized phase. The maximum at 217°C for natural chrysocolla corresponds to the maximum at 230°C for the sample synthesized at 25°C. The weak shift towards lower values (217°C) is well accounted for by the lower hydrogen partial pressure in our experiments (5% H_2/Ar mixture instead of 10% H_2/Ar) [21]. When a 5% H_2/Ar mixture was used to reduce natural chrysocolla [13] the TPR maximum was found to occur at 235°C.

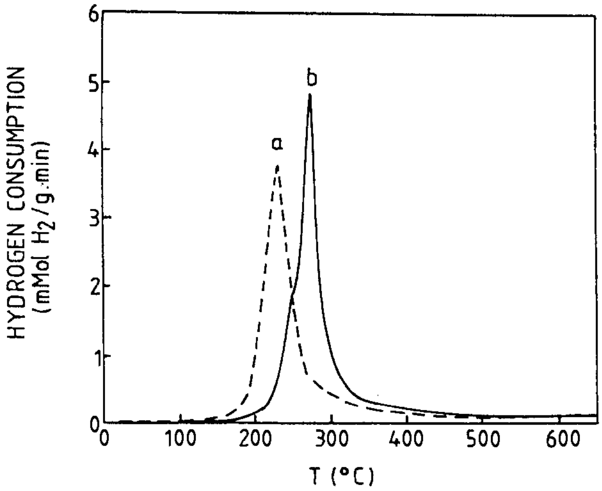

Fig. 5. TPR profiles of chrysocolla synthesized at (a) 25°C, (b) 80°C.

In contrast to Ni-talcs, the TPR profiles for chrysocolla appear quite symmetric and sharper, probably indicating a narrower distribution of particle sizes. Silica supported Cu samples also exhibit sharp profiles [12], contributing to an easier identification of the supported phase.

Because TPR maxima in different natural copper minerals are found in separate temperature ranges (TPR maxima for dioptase are observed 200°C higher than for chrysocolla) and because these materials are particularly ill-crystallized, the identification from TPR profiles of silica supported Cu catalysts with chrysocolla was in this case reliable.

How can we explain the better reducibility of chrysocolla in comparison to Ni-talc as shown by their respective TPR maxima (230 and 470°C for the materials synthesized at 25°C)? Several parameters occur in the reduction process of a transition metal ion containing compound. For a given transition metal ion, the nature of the phyllosilicate intervenes: thus Ni phyllosilicates of 1 : 1 type (nepouite-like structure) are found to be more reducible than Ni phyllosilicates of 2 : 1 type (talc-like structure) [15], owing to the better accessibility of the octahedral sheet which is directly exposed to hydrogen. On the other hand, the proximity of structural OH groups in the octahedral layer of nepouite (fig. 1b), makes the dehydroxylation process easier for this phyllosilicate in comparison to talcs where OH groups are separated by SiO_4 tetrahedra (fig. 1a). For a given compound, the reducibility of the transition metal ion has also to be taken into account. Thus thermodynamic data suggest that CuO is more easily reduced than NiO as indicated by the values of ΔG^0 for the formation of NiO and CuO [27] ($\Delta G^0_{NiO} = -12$ kJ mol^{-1} and $\Delta G^0_{CuO} = -101$ kJ mol^{-1}) and this is in agreement with their TPR maxima observed at 400 and 300°C respectively. Finally, the particular structure of chrysocolla with discontinuous sheets of Cu octahedra gives rise to channels (fig. 1c), also contributing to an easier access to hydrogen. All these factors may account for the differences in the reducibility of these materials.

5. Conclusion

This study was carried out with the aim of identifying silica-supported layered silicates produced during the preparation of Ni/SiO_2 and Cu/SiO_2 catalysts. A set of pure reference compounds Ni-talc and chrysocolla were synthesized at various temperatures and investigated using XRD and TPR. The degree of crystallinity of the Ni phyllosilicates was shown to increase with the temperature of synthesis in contrast to chrysocolla samples which remained ill-organized. In the case of Ni phyllosilicates, the marked asymmetry of the TPR profiles towards lower temperatures has been discussed in connection with the phase boundary-controlled reaction model developed by Lemaitre [21]. This model could be applied provided that there is a heterogeneous distribution of the clay particle sizes. A significant proportion of particles of smaller size for synthesis temperatures lower than 250°C accounts for the shapes of the corresponding talcs. In this respect, Ta_{150} exhibits the highest fraction of particles of smaller size. At 500°C, the talc is well crystallized and the distribution is narrower and shifted towards particles of larger size.

Our results, in line with those of Lemaitre and Gérard [15], emphasize the influence of the crystallinity of phyllosilicates on their reducibility. It appears first that well-crystallized synthetic silicates as reference compounds should be preferred to ill-crystallized natural minerals. On the other hand, the crystallinity degree is a parameter to be taken into account for the identification of supported silicates. Indeed, the preparation method and the experimental conditions (pH of the solution, nature of the Ni salt, ageing, hydrothermal treatment) may influence the degree of crystallinity of the supported Ni silicate and therefore the position of the TPR peak. Thus, the identification of the supported silicate by TPR only appears questionable. The use of several complementary techniques such as FTIR, EXAFS and TEM is highly recommended. In the case of Ni, EXAFS [8,9] and FTIR [9,24] were found to be relevant tools to determine the nature of the supported silicate (talc or nepouite). These investigations may be extended to other systems where supported phyllosilicates are produced.

Acknowledgement

The authors gratefully acknowledge Dr. J.L. Robert (CRSCM-CNRS Orleans) for the synthesis and the X-ray diffractogram of Ta_{500} and thank Dr. P. Burattin (Laboratoire de Réactivité de Surface et Structure, URA 1106 CNRS, Paris) for computerizing the TPR apparatus and for stimulating discussions.

References

[1] M. Che and L. Bonneviot, in: *Successful Design of Catalysts*, ed. T. Inui (Elsevier, Amsterdam, 1988) p. 147;
M. Che, *Proc. 10th Int. Congr. on Catalysis*, eds. L. Guczi, F. Solymosi and P. Tétényi (Akadémiai Kiado, Budapest, 1993) p. 31.

[2] J.W.E. Coenen and B.G. Linsen, in: *Physical and Chemical Aspects of Adsorbents*, ed. B.G. Linsen (Academic Press, London, 1970) p. 471.

[3] J.A. Van Dillen, J.W. Geus, L.A.M. Hermans and J. Van Der Meuden, *Proc. 6th Int. Congr. on Catalysis*, eds. G.C. Bond, P.B. Wells and F.C. Tompkins (The Chemical Society, London, 1977) p. 677.

[4] L.A.M. Hermans and J.W. Geus, in: *Preparation of Catalysts II*, eds. B. Delmon, P. Grange, P. Jacobs and G. Poncelet (Elsevier, Amsterdam, 1979) p. 113.

[5] J.T. Richardson, R.J. Dubus, J.G. Crump, P. Desai, U. Osterwalder and T.S. Cale, in: *Preparation of Catalysts II*, eds. B. Delmon, P. Grange, P. Jacobs and G. Poncelet (Elsevier, Amsterdam, 1979) p. 131.

[6] M. Houalla, F. Delannay, I. Matsuura and B. Delmon, J. Chem. Soc. Faraday Trans. 76 (1980) 2128.

[7] R. Burch and A.R. Flambard, in: *Preparation of Catalysts III*, eds. G. Poncelet, P. Grange and P.A. Jacobs (Elsevier, Amsterdam, 1983) p. 311.
[8] O. Clause, L. Bonneviot, M. Che and H. Dexpert, J. Catal. 130 (1991) 21.
[9] O. Clause, M. Kermarec, L. Bonneviot, F. Villain and M. Che, J. Am. Chem. Soc. 114 (1992) 4709.
[10] Z.X. Cheng, C. Louis and M. Che, Z. Phys. 20 D (1991) 445.
[11] A. Jones and B.D. McNicol in: *Temperature-Programmed Reduction for Solid Materials Characterization*, Chemical Industries Series, Vol. 24 (Dekker, New York, 1986).
[12] G.J.C. van der Grift, A. Mulder and J.W. Geus, Appl. Catal. 60 (1990) 181.
[13] G.J.C. van der Grift, A.F.H. Wielers, A. Mulder and J.W. Geus, Thermochim. Acta 171 (1990) 95.
[14] G.A. Martin, B. Imelik and M. Prettre, J. Chim. Phys. 66 (1969) 1682.
[15] J.Lemaitre and P. Gérard, Bull. Miner. 104 (1981) 655.
[16] G.W. Brindley and G. Brown, in: *Crystal Structure of Clay Minerals and their X-Ray Identification* (Mineralogical Society, London, 1980) (a) p. 2, (b) p. 165, (c) p. 131.
[17] F.V. Chukhrov, B.B. Zvyagin, L.P. Ermilova, A.I. Gorshov and E.S. Rudnitskaya, *Proc. Int. Clay. Conf.,* Tokyo 1 (1969) 141.
[18] M.C. Van Oosterwyck-Gastuche, Compte Rend. Acad. Sci. Paris D 271 (1970) 1837.
[19] A. Decarreau, Bull. Miner. 103 (1980) 579.
[20] A. Decarreau, Geochim. Cosmochim. Acta 49 (1985) 1537.
[21] J.L. Lemaitre, in: *Characterization of Heterogeneous Catalysts*, ed. F. Delannay (Dekker, New York, 1984) p. 29.
[22] J. Sestak, V. Savata and W.W. Wendtland, Thermochim. Acta 7 (1973) 333.
[23] B. Delmon, in: *Introduction à la Cinétique Hétérogène* (Technip, Paris, 1969) pp. 277–321.
[24] M. Kermarec, J.Y. Carriat, M. Che and A. Decarreau, to be published.
[25] G. Wendt and M. May, Z. Chem. 26 (1986) 117.
[26] J.W.E. Coenen, Appl. Catal. 54 (1989) 65.
[27] C.W. Robert and J.A. Melvin, eds., *Handbook of Chemistry and Physics* (CRC Press, Boca Raton, 1980/1981).